THE JOURNAL OF BIOLOGICAL CHEMISTRY
Vol. 271, No. 20, Issue of May 17, pp. 11710–11717, 1996
Printed in U.S.A.

Phosphorylation of the *InaD* Gene Product, a Photoreceptor Membrane Protein Required for Recovery of Visual Excitation*

(Received for publication, January 11, 1996)

Armin Huber‡, Philipp Sander, and Reinhard Paulsen

From the Zoological Institute I, University of Karlsruhe, 76128 Karlsruhe, Germany

In an approach directed to isolate and characterize key proteins of the transduction cascade in photoreceptors using the phosphoinositide signaling pathway, we have isolated the *Calliphora* homolog of the *Drosophila InaD* gene product, which in *Drosophila InaD* mutants causes slow deactivation of the light response. By screening a retinal cDNA library with antibodies directed against photoreceptor membrane proteins, we have isolated a cDNA coding for an amino acid sequence of 665 residues (M_r = 73,349). The sequence displays 65.3% identity (77.3% similarity) with the *Drosophila InaD* gene product. Probing Western blots with monospecific antibodies directed against peptides comprising amino acids 272–542 (anti-*InaD*-(272–542)) or amino acids 643–655 (anti-*InaD*-(643–655)) of the *InaD* gene product revealed that the *Calliphora InaD* protein is specifically associated with the signal-transducing rhabdomeral photoreceptor membrane from which it can be extracted by high salt buffer containing 1.5 M NaCl. As five out of eight consensus sequences for protein kinase C phosphorylation reside within stretches of 10–16 amino acids that are identical in the *Drosophila* and *Calliphora InaD* protein, the *InaD* gene product is likely to be a target of protein kinase C. Phosphorylation studies with isolated rhabdomeral photoreceptor membranes followed by *InaD* immunoprecipitation revealed that the *InaD* protein is a phosphoprotein. *In vitro* phosphorylation is, at least to some extent, Ca^{2+}-dependent and activated by phorbol 12-myristate 13-acetate. The *inaC*-encoded eye-specific form of a protein kinase C (eye-PKC) is co-precipitated by antibodies specific for the *InaD* protein from detergent extracts of rhabdomeral photoreceptor membranes, suggesting that the *InaD* protein and eye-PKC are interacting in these membranes. Co-precipitating with the *InaD* protein and eye-PKC are two other key components of the transduction pathway, namely the *trp* protein, which is proposed to form a Ca^{2+} channel, and the *norpA*-encoded phospholipase C, the primary target enzyme of the transduction pathway. It is proposed that the rise of the intracellular Ca^{2+} concentration upon visual excitation initiates the phosphorylation of the *InaD* protein by eye-PKC and thereby modulates its function in the control of the light response.

Phototransduction by rhabdomeral photoreceptors, particularly of *Drosophila* compound eyes, has become an important model system for the ubiquitous phosphoinositide-mediated signal transduction. The progress achieved in this field is based on the powerful genetic and molecular biological techniques available for *Drosophila*, which have been successfully complemented by biochemical studies in other flies such as *Calliphora* and *Musca*. Despite the rapid progress that has been achieved in the understanding of sensory transduction mechanisms in recent years, the phototransduction cascade operating in this type of sensory cells has not yet been entirely resolved. In particular, the biochemical processes regulating the recovery and adaptation of the visual response in rhabdomeral photoreceptors are still obscure.

Extracellular Ca^{2+} enters the photoreceptors through ion channels and is required for rapid recovery of visual excitation (1–5). A major portion of the Ca^{2+} influx into the photoreceptor cell appears to be carried by a Ca^{2+}-selective class of channels that depend on, or may indeed be formed by, the transient receptor potential (*trp*)[1] protein (6, 7). The primary structure of this *trp* protein was identified simultaneously by Wong *et al.* (8) and Montell and Rubin (9), and the *trp* gene product was shown to be localized to the rhabdomeral photoreceptor membranes. Direct measurements of the extracellular Ca^{2+} concentration revealed a decline of extracellular Ca^{2+} upon illumination in the eyes of wild type flies, which is significantly reduced in *trp* mutants (4). Signal transduction is also impaired in two other *Drosophila* mutants, *inaC* and *InaD*, which were originally classified as inactivation-no afterpotential mutants by Pak (10). While the *InaD* gene product is an 80-kDa protein of unknown function (11), the *inaC* gene was shown to encode an eye-specific protein kinase C (eye-PKC) (12, 13). Thus, it is tempting to assume that the Ca^{2+}-dependent deactivation of the visual response is controlled by phosphorylation of photoreceptor-specific proteins associated with the rhabdomeral photoreceptor membrane. Identified proteins that undergo light-dependent phosphorylation are rhodopsin and arrestin 2 (14–17). However, neither rhodopsin nor arrestin 2 were found to be phosphorylated by the *inaC* protein because phosphorylation of activated rhodopsin is not enhanced by Ca^{2+} (14, 15), and the Ca^{2+}-stimulated phosphorylation of arrestin 2 has been shown to result from the activation of a Ca^{2+}-calmodulin-dependent protein kinase (17). Accordingly, the target proteins of eye-specific protein kinase C have yet to be specified.

In an attempt to identify proteins that are part of the biochemical pathway in rhabdomeral photoreceptors, we have used an immunological approach to isolate *Calliphora* cDNA clones, which encode photoreceptor membrane proteins. Antibodies directed against purified rhabdomeral membranes (18)

* This work was supported by funds provided by the Deutsche Forschungsgemeinschaft, Pa 274/3–4. The costs of publication of this article were defrayed in part by the payment of page charges. This article must therefore be hereby marked "*advertisement*" in accordance with 18 U.S.C. Section 1734 solely to indicate this fact.

The nucleotide sequence from which the amino acid sequence reported in this paper was deduced has been submitted to the GenBank™/EMBL Data Bank with accession number Z69883.

‡ To whom correspondence and reprint requests should be addressed: Universität Karlsruhe, Zoologisches Institut I, Postfach 6980, 76128 Karlsruhe, Germany. Tel.: 721-6082218; Fax: 721-6084848.

[1] The abbreviations used are: *trp*, transient receptor potential; *inaC*, inactivation-no afterpotential C; *InaD*, inactivation-no afterpotential D; *norpA*, no receptor potential A; PAGE, polyacrylamide gel electrophoresis.

were generated and employed for the isolation of genes encoding rhabdomere-specific proteins. By this approach, we have cloned the *Calliphora* homologs of the *Drosophila InaD*, *inaC*, and *trp* genes. In the present paper we show that the *InaD* gene product is associated with the rhabdomeral photoreceptor membrane and that it is a putative substrate of eye-PKC. We also provide for the first time evidence for an interaction among eye-PKC, *InaD* protein, *trp* protein, and the *norpA*- (no receptor potential A) encoded phospholipase C.

EXPERIMENTAL PROCEDURES

Fly Stocks—Calliphora erythrocephala Meig., chalky mutant, was reared on bovine liver to maintain a high rhodopsin content in the eyes. Adult male flies were raised at 25 °C in a 12 h light/12 h dark cycle and were used for the experiments at an age of 8–10 days posteclosion.

Generation of Antibodies—Immunization of rabbits was performed according to standard protocols (19). Isolated rhabdomes of 700 *Calliphora* eyes were used for each of the four injections. Final blood sampling was 4 months after the first injection. The obtained antiserum was purified on protein A-agarose columns (Bio-Rad Life Technologies, Munich) as described (19).

Polyclonal anti-*InaD* antibodies were generated as follows: a DNA fragment encoding the 23 C-terminal amino acids of the *Calliphora InaD* protein was amplified by polymerase chain reaction from cloned cDNA using sequence-specific primers. The polymerase chain reaction product was cloned into the expression vector pQE40 (Qiagen, Hilden/Germany) in frame with six His codons and the dihydrofolate reductase gene. Fusion proteins were expressed in *Escherichia coli* M15 (pREP4), extracted with urea and purified on Ni^+-agarose columns according to the manufacturer's instructions. Purified fusion proteins were dialyzed against phosphate-buffered saline (137 mM NaCl, 3 mM KCl, 8 mM Na_2HPO_4, 2 mM KH_2PO_4, pH 7.2) and used for the immunization of a rabbit (200 μg of protein/injection). Antibodies were purified from the antiserum by affinity chromatography on HiTrap columns (Pharmacia, Freiburg/Germany), which had previously been coupled with 1 mg of the antigen as described by the manufacturer. The purified antibodies are hereafter referred to as anti-*InaD*-(643–665), according to the *InaD* peptide from which they were raised. A second anti-*InaD* antibody (anti-*InaD*-(272–542)) was generated and purified in the same way by using a recombinantly expressed peptide comprising amino acids 272–542 of the *Calliphora InaD* protein.

For the production of anti-*Calliphora trp* antibodies a partial *Calliphora* cDNA clone encoding the C-terminal half of the *trp* protein was expressed in *E. coli* M15 (pREP4), and the expression product was used as an antigen. Antibodies directed against the *Calliphora inaC* protein and the α-subunit of the eye-specific G-protein were raised against bovine serum albumin-coupled synthetic peptides (CYMNPEFITMI and QNALKEFNLG, respectively), which correspond to the C-terminal region if these proteins. Antibodies directed against the *Drosophila norpA*-encoded phospholipase C and against the β-subunit of the G-protein, which also detect the corresponding *Calliphora* proteins, were a generous gift of R. Shortridge (20) and J. B. Hurley (21).

Construction of a Calliphora Retinal cDNA Library, Immunoscreening, and Sequencing—A *Calliphora* retinal cDNA library was prepared in the UniZAP XR vector (Stratagene, Heidelberg/Germany) according to the manufacturer's instructions, using poly(A)$^+$ RNA isolated from 500 *Calliphora* retinae. Screening of the library with antibodies against rhabdomeral proteins was performed as described by Sambrook *et al.* (22). Expression of recombinant proteins was induced by applying nitrocellulose filters preincubated in 1 mM isopropyl-β-D-thiogalactopyranoside 3 h after plating the phages. After an additional incubation for 4 h at 37 °C the filters were removed from the plates, washed briefly in Tris-buffered saline (20 mM Tris/HCl, pH 7.5, 150 mM NaCl), blocked for 2 h at 25 °C in 3% bovine serum albumin in Tris-buffered saline, and incubated overnight at 25 °C in the same solution containing $^1/_{1000}$ volume of antiserum. Binding of primary antibodies was detected using alkaline phosphatase-conjugated protein A and with nitro blue tetrazolium/X-phosphate as a chromogen. Positive clones were rescreened, and plasmid DNA was obtained by *in vivo* excision. The nucleotide sequence of the longest cDNA clone was determined for both strands by the dideoxy chain termination method (23) using templates generated by nested deletions.

Isolation of Photoreceptor Membranes, SDS-PAGE, and Western Blot Analysis—Isolation of total eye membranes and rhabdomeral photoreceptor membranes was performed as described previously (15, 18). Low salt extractions were carried out in 3 mM EGTA, 1 mM dithiothreitol in 5 mM sodium phosphate buffer, pH 6.2, for 10 min on ice. 50 mM sodium phosphate buffer, pH 6.2, containing 1.5 M NaCl was used for high salt extractions of purified photoreceptor membranes. After complementing extracts with 5 × SDS-PAGE buffer (1 × SDS-PAGE buffer: 4% SDS, 1% 2-mercaptoethanol, 1 mM EDTA, 15% glycerol in 65 mM Tris/HCl, pH 6.8) or solubilizing membrane proteins in 1 × SDS-PAGE buffer, the proteins were separated by SDS-PAGE according to Laemmli (24) on 8–20% gradient gels (Pharmacia Midget System). Following SDS-PAGE, proteins were transferred to polyvinylidene difluoride membranes (Bio-Rad), and Western blot analysis was performed using standard protocols (19).

Immunoprecipitation of the InaD Protein—Proteins were extracted from purified rhabdomeral membranes of 30 *Calliphora* eyes in 30 μl of Triton X-100 buffer (1% Triton X-100, 150 mM NaCl, 50 mM Tris/HCl, pH 8.0, and 1 mM phenylmethylsulfonyl fluoride) for 15 min at 4 °C. The extract was added to 10 μl of protein A/G-agarose beads (Pierce), which had previously been incubated with anti-*InaD*-(272–542) for 1 h. Immunoprecipitation was performed for 2 h at 4 °C and was followed by four washes with 500 μl of Triton X-100 buffer. Precipitated proteins were eluted from protein A/G-agarose beads with 15 μl of 1 × SDS-PAGE buffer for 10 min at 80 °C and were subjected to SDS-PAGE and Western blot analysis.

Protein Phosphorylation and Dephosphorylation—The standard assay for protein phosphorylation was carried out in a buffer containing Hepes-buffered saline (115 mM NaCl, 2 mM KCl, 10 mM Hepes), pH 6.8, 2 mM $MgCl_2$, 1 mM dithiothreitol, 1 mM phenylmethylsulfonyl fluoride, 125 μM EGTA, 250 μM $CaCl_2$, and purified photoreceptor membranes from 10 fly retinae per sample. When indicated, phorbol 12-myristate 13-acetate or bisindolylmaleimide I (Calbiochem, Bad Soden/Germany) were added at a final concentration of 1 μM or 0.2 μM, respectively. The phosphorylation reactions were started by the addition of 2 mM ATP supplemented with 2 μCi [γ-^{32}P]ATP (Amersham Buchler, Braunschweig). The free Ca^{2+} concentration in these assays, calculated according to Fabiato (25), was 60 μM. Phosphorylation reactions that contained nominally zero Ca^{2+} were supplemented with 2 mM EGTA to remove internal Ca^{2+}, and no external Ca^{2+} was added. The soluble fraction of retinal proteins used in recombination experiments was obtained by homogenizing retinae in a small volume (about 0.5 μl/retina) of 1 mM phenylmethylsulfonyl fluoride in water and subsequently separating the soluble and particulate fraction by centrifugation at 50,000 × *g* for 10 min. Aliquots of soluble proteins of six retinae were added per sample in recombination experiments. Rhabdomeral photoreceptor membranes were prepared under dim red light. For activating light-dependent metarhodopsin phosphorylation, samples were illuminated with blue light for 2 min immediately before the reactions were started. In some cases blue light illumination was omitted as noted in the figure legends. If not indicated otherwise, the phosphorylation was carried out for 5 min at 20 °C in the dark. Thereafter, membranes were sedimented at 13,000 × *g* at 4 °C for 10 min, and proteins were extracted with high salt buffer, Triton X-100 buffer, or SDS-PAGE buffer and were subjected to SDS-PAGE or were immunoprecipitated as described above. For measuring phosphorylation time courses, reactions were terminated by adding 5 × SDS-PAGE buffer at the indicated times, and the whole sample was subjected to SDS-PAGE. The amount of protein loaded was visualized by staining the gels with Coomassie Blue, and protein phosphorylation was detected by autoradiography using Kodak BiomaxMR films. Quantification of the relative amount of radioactivity present in a protein band was performed with a phosphor imager (FUJIX BAS 1000, Fuji). For determining the stoichiometry of phosphorylation the radioactivity of cut-out protein bands was measured in a scintillation counter. The amount of *InaD* protein present in the *InaD* protein band was calculated by laser densitometry using bovine serum albumin as a standard.

RESULTS

Isolation and Characterization of Calliphora InaD cDNAs—Antibodies directed against proteins of the fly photoreceptor membrane had been generated by immunizing rabbits with rhabdomes (*i.e.* a subcellular fraction composed of the rhabdomeral photoreceptor membranes and the intraommatidial matrix; see Ref. 18) isolated from 2800 *Calliphora* eyes. The resulting antiserum was used to immunoscreen a *Calliphora* retinal cDNA library. Out of 280,000 clones screened, 200 clones expressed polypeptides that reacted with the antiserum. Partial sequencing analysis revealed that the positive clones isolated so far encode at least six different proteins.

Work presented in this study focuses on clones that show homology to the recently published *Drosophila InaD* gene (11).

We obtained 14 cDNA clones coding for the *Calliphora* homolog of *InaD* and determined the nucleotide sequence of the longest cDNA for both strands. This clone contained a 201-base pair 5′-untranslated region, a 1995-base pair open reading frame encoding a polypeptide of 665 amino acids (M_r = 73,349), and a 194-base pair 3′-untranslated region. The translation initiation site was assigned arbitrarily to the first AUG of the open reading frame at nucleotide 202, which is preceded by a stop codon at nucleotide 196, and fits well with the consensus sequence for translation initiation sites in *Drosophila*, (C/A)AA(A/C)AUG (26). Alignment of the deduced amino acid sequence of the *Calliphora* cDNA clone with the *Drosophila InaD* sequence (Fig. 1*a*) shows that the two proteins display 65.3% overall amino acid identity and 77.3% similarity if conservative substitutions are taken into account. Furthermore, both proteins share similar biophysical characteristics, *i.e.* the same predicted isoelectric point of 8.6, a high abundance of basic (Lys, Arg, His) and acidic (Asp, Glu) amino acids that together comprise more than 30% of the polypeptide, and similar hydrophilicity profiles (Fig. 1*b*) that reveal no stretches of hydrophobic sequences of 20 or more residues in length.

Two repeats of 40 amino acids (*underlined* in Fig. 1*a*) that were shown to share limited sequence homology with the *Drosophila* disc-large (Dlg), the rat post-synaptic density protein (PSD95), the vertebrate tight junction protein ZO-1, and the human ROS protein (see Ref. 11 and references therein), are highly conserved (90% similarity) between the *Calliphora* and *Drosophila InaD* proteins, implying a common functional role within the family of proteins that contain these repeats. On the other hand, repeats consisting of Gly-(Gln/Met), which are present in the *Drosophila InaD* sequence between amino acids 142 and 158, are not found in the *Calliphora* sequence. Indeed, the region between residues 106 and 183 is the least conserved part of the two proteins. The only common feature within this region is the relatively high abundance of glutamine residues. Another striking sequence motif, which is present in the *Calliphora* and the *Drosophila InaD* protein, is the highly hydrophilic cluster of lysine and glutamate residues between amino acids 454 and 473 (indicated by *bars* in Fig. 1*b*). While potential phosphorylation sites of cAMP- and cGMP-dependent protein kinase and tyrosine kinase present in the *Drosophila* sequence at Thr^{169} and Tyr^{203}, respectively, are not found in the *Calliphora* sequence, eight potential phosphorylation sites of protein kinase C are conserved (Fig. 1*a*). Finally, two potential glycosylation sites at Asn^{168} and Asn^{312} (*Drosophila*) or Asn^{162} and Asn^{303} (*Calliphora*) are found at similar positions in both sequences.

Identification and Localization of the InaD Protein by Monospecific Antibodies—In order to obtain more detailed information on the function of *InaD* in fly phototransduction, it is crucial to know whether the *InaD* gene product is a membrane protein, and if so whether it resides in the rhabdomeral membrane. Isolation of the *InaD* clone by means of an anti-rhabdom serum already suggests that the *InaD* protein is associated either with rhabdomeres or with the intraommatidial (extracellular) matrix of the photoreceptor cells. The *InaD* protein was identified on Western blots using monospecific anti-*InaD*-(643–665) and anti-*InaD*-(272–542) antibodies that were raised against peptides containing the 23 C-terminal amino acids and amino acids 274–542 of the *Calliphora InaD* protein, respectively. Both antibodies bind to a single protein with an apparent molecular mass of 75 kDa (Fig. 2). The apparent molecular mass of 75 kDa is in line with the molecular mass deduced from the cDNA sequence (73,349 Da). This demonstrates that the *InaD* protein is present in total eye membranes and in purified photoreceptor membranes (Fig. 2, *lanes 1* and *3*). It is detected neither in the fraction containing soluble proteins obtained from whole retinas after extraction with low salt buffer nor in extracts containing proteins of the intraom-

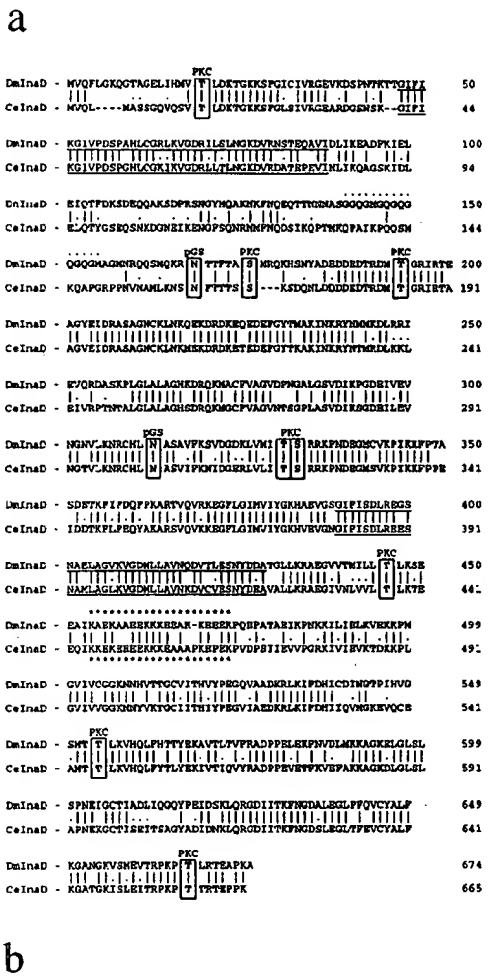

FIG. 1. **Comparison of the primary structure of the *Drosophila* and *Calliphora InaD* protein.** *a*, alignment of the deduced amino acid sequences of the *Drosophila* and *Calliphora InaD* gene products. Amino acids are shown in single-letter code. Amino acid identities and similarities between the two proteins are indicated by *vertical bars* and *points*, respectively. *Boxed* serine and threonine residues represent potential protein kinase C phosphorylation sites (*PKC*), and *boxed* asparagine residues indicate potential *N*-glycosylation sites (*pGS*). Two conserved repeats are *underlined*. G-(Q/M) repeats that are present only in the *Drosophila InaD* protein between amino acids 141 and 155 are indicated by a *dotted line*. A lysine/glutamate-rich cluster is labeled by *stars*. *b*, hydrophilicity profile (window size: 7) of the *Drosophila* and *Calliphora InaD* protein according to Kyte and Doolittle (46). The *arrow* depicts the position of Met^{442}, which is replaced by a lysine in $InaD^{P215}$ mutants. *Bars* indicate the position of lysine/glutamate-rich clusters.

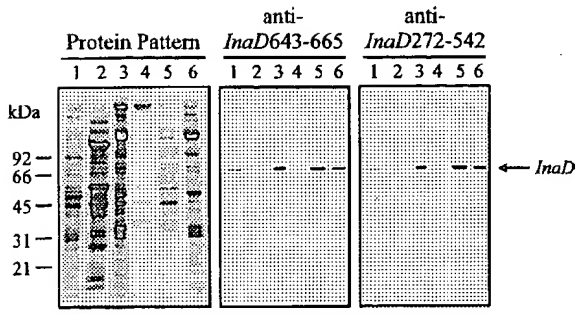

FIG. 2. **Immunoblot analysis of the *InaD* protein.** Retinal proteins were separated by SDS-PAGE and stained with Coomassie Blue (*left panel*) or transferred onto a polyvinylidene difluoride membrane for immunological detection with antibodies directed against the C-terminal region of the *InaD* protein (anti-*InaD*-(643–665)) or a peptide comprising amino acids 272–542 (anti-*InaD*-(272–542)). Membrane and soluble proteins from one *Calliphora* retina were analyzed in *lanes 1* and *2*, respectively. Proteins extracted with 1 × SDS-PAGE buffer from purified photoreceptor membranes of 10 *Calliphora* eyes were loaded on *lane 3*. *Lanes 4–6* show rhabdomeral proteins obtained after subsequently extracting purified photoreceptor membranes with a low salt buffer containing 3 mM EGTA (*lane 4*) with a high salt buffer containing 1.5 M NaCl (*lane 5*) and with 1 × SDS-PAGE buffer (*lane 6*).

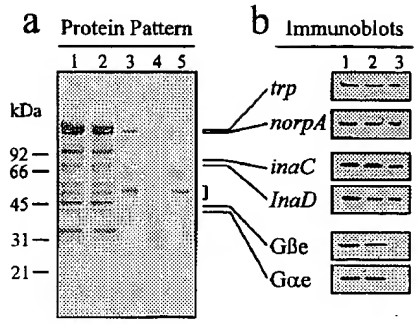

FIG. 3. **Co-immunoprecipitation of the *InaD*, *InaC*, *trp*, and *norpA* proteins.** Rhabdomeral proteins were extracted with Triton X-100 buffer, immunoprecipitated with anti-*InaD*-(272–542) and subjected to SDS-PAGE and Western blot analysis. *a*, Coomassie-stained gel showing the proteins extracted with Triton X-100 buffer from rhabdomeral membranes of 10 eyes (*lane 1*), the proteins that are not immunoprecipitated by anti-*InaD*-(272–542) (*lane 2*; equivalent of 10 eyes), and the proteins present in the immunoprecipitates (*lane 3*; equivalent of 30 eyes). *Lanes 4* and *5* show control experiments. When protein A/G-agarose beads without antibody were used in the immunoprecipitation experiment, no immunoprecipitates were obtained (*lane 4*). On *lane 5* anti-*InaD*-(272–542) eluted from protein A-Sepharose beads was loaded in order to identify protein bands, which represent the antibodies (indicated by *bracket*). *b*, Western blots of the proteins shown in *lanes 1–3* of *panel a* were probed with anti-*InaD*-(643–665) and with antibodies specific for the *trp*, *norpA*, and *inaC* proteins and for the α- and β-subunits of an eye-specific G-protein ($G_{\alpha e}$ and $G_{\beta e}$, respectively).

matidial matrix (Fig. 2, *lanes 2* and *4*). The latter extract was prepared by extraction of purified photoreceptor membranes with a low salt buffer containing EGTA. However, the *InaD* protein is extracted from the rhabdomeral photoreceptor membrane if a high salt buffer containing 1.5 M NaCl is used (Fig. 2, *lane 5*). As is expected using this cloning procedure, the Western blot indicates that the *InaD* protein is enriched in the photoreceptor membrane preparation as compared with total eye membranes. Taken together, the hydrophilic character of the *InaD* protein predicted by the sequence data, and its solubilization by a high salt buffer reveals that *InaD* is a peripheral photoreceptor membrane protein.

Purification of the InaD Protein by Immunoprecipitation—In order to purify the *InaD* protein by immunoprecipitation rhabdomeral membranes were treated with a buffer containing 1% Triton X-100, which quantitatively extracted the *InaD* protein from nonsoluble material. Anti-*InaD*-(643–665) failed to immunoprecipitate the *InaD* protein. Thus, we generated an antiserum that was directed against a different part of the *InaD* protein (anti-*InaD*-(272–542)) and could successfully be used for immunoprecipitation (Fig. 3). Resolving the immunoprecipitates obtained with anti-*InaD*-(272–542) by SDS-PAGE revealed that, in addition to the *InaD* protein band, two other protein bands with apparent molecular masses of 140 and 80 kDa were immunoprecipitated (Fig. 3*a*, *lane 3*). None of these proteins was precipitated in control experiments in which protein A/G beads alone were used (Fig. 3*a*, *lane 4*). The 140-kDa protein band turned out to represent a double band when resolved on 8% polyacrylamide gels (data not shown). Western blot analysis (Fig. 3*b*) showed that this protein band reacted with antibodies specific for the *Calliphora trp* protein and for the *norpA*-encoded phospholipase C. The 80-kDa protein represents the eye-specific protein kinase C (*inaC* protein). The immunoprecipitates were also probed with antibodies specific for the α- and β-subunit of an eye-specific G-protein. These G-protein subunits were not detected in the immunoprecipitates. Since anti-*InaD*-(272–542) does not cross-react with rhabdomeral proteins other than the *InaD* protein on Western blots, the co-precipitation of *inaC*, *trp*, and *norpA* proteins by anti-*InaD*-(272–542) suggests that these proteins are complexed permanently or transiently with the *InaD* protein in the photoreceptor membranes.

Phosphorylation of the Calliphora InaD Protein—The co-immunoprecipitation of the *InaD* protein with an eye-specific protein kinase C prompted us to investigate whether or not the *InaD* gene product is a phosphoprotein. In order to test this hypothesis, we made use of the ability to enrich the protein by high salt extraction of purified photoreceptor membranes. In the experiment depicted in Fig. 4, the *InaD* protein was extracted with high salt buffer after performing phosphorylation of photoreceptor membrane proteins under the standard conditions described under "Experimental Procedures." The extracted peripheral proteins, as well as integral membrane proteins, were subjected to SDS-PAGE and autoradiographed. Of the seven protein bands detected in the high salt extract after staining the gel with Coomassie Blue, four proteins are phosphorylated. The most prominent of these phosphoproteins shows an apparent molecular mass of about 75 kDa, a value corresponding to the apparent molecular mass of the *InaD* protein. Autoradiography of a duplicate blot and subsequent probing of the very same blot with anti-*InaD*-(643–665) demonstrated that the radioactively labeled protein band at 75 kDa represents the *InaD* protein band (Fig. 4*b*). In order to rule out that a phosphoprotein other than the *InaD* protein is present in the high salt extracts and has the same electrophoretic mobility as the *InaD* protein upon separation by SDS-PAGE, phosphorylated *InaD* protein was also purified by immunoprecipitation (Fig. 5). The presence of radioactive phosphate in the 75-kDa protein band, which was obtained by resolving the anti-*InaD*-(272–542) immunoprecipitates by SDS-PAGE and which was identified as the *InaD* protein with anti-*InaD*-(643–665), clearly demonstrated that the *InaD* protein is a phosphoprotein. The stoichiometry of *InaD* protein phosphorylation, determined for the *InaD* protein present in high salt extracts as described under "Experimental Procedures," was 0.4–0.5 mol of phosphate/mol of *InaD* protein. Hence, a substantial fraction of the *InaD* molecules was not phosphorylated in the *in vitro* assays, which may indicate that a fraction of *InaD* molecules is isolated in a phosphorylated form or is compartmentalized in membrane vesicles to which externally added ATP or activators of the protein kinase have no access.

Since eye-PKC co-immunoprecipitating with the *InaD* pro-

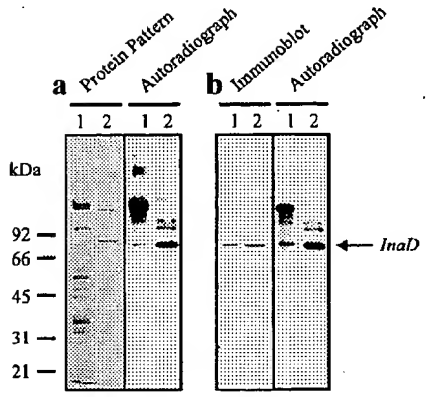

FIG. 4. **Identification of phosphorylated *InaD* protein.** In order to demonstrate phosphorylation of the *InaD* gene product, proteins of dark-adapted rhabdomeral membranes that remained in the membrane fraction after extraction with low salt buffer containing 3 mM EGTA were phosphorylated in the presence of 2 μCi of [γ-^{32}P]ATP as described under "Experimental Procedures." After phosphorylation the *InaD* protein was extracted from the membrane with high salt buffer. Membrane proteins that were not extracted under these conditions were solubilized with SDS-PAGE buffer. The aliquots equivalent to purified photoreceptor membranes of 10 retinae for the SDS extract or 40 retinae for the high salt extract were subjected to SDS-PAGE. *a*, Coomassie-stained protein pattern and corresponding autoradiograph of the SDS-extracted proteins (*lane 1*) and the high salt-extracted proteins (*lane 2*). *b*, immunoblot of the same extracts as shown in *panel a* probed with anti-*InaD*-(643–665) and corresponding autoradiograph.

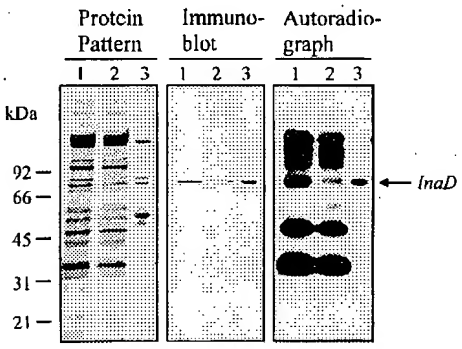

FIG. 5. **Immunoprecipitation of phosphorylated *InaD* protein.** Proteins of blue light-illuminated rhabdomeral membranes were phosphorylated in the presence of 2 μCi of [γ-^{32}P]ATP as described under "Experimental Procedures." Then the rhabdomeral membrane proteins were extracted with Triton X-100 buffer and subjected to immunoprecipitation with anti-*InaD*-(272–542). Proteins of the Triton X-100 extract (*lane 1*), of the supernatant containing the nonprecipitated proteins (*lane 2*), and of the immunoprecipitates (*lane 3*) were resolved by SDS-PAGE and subjected to Western blot analysis and autoradiography. The Coomassie-stained protein gel, the immunoblot probed with anti-*InaD*-(643–665), and the autoradiograph of the immunoblot are shown from *left* to *right*.

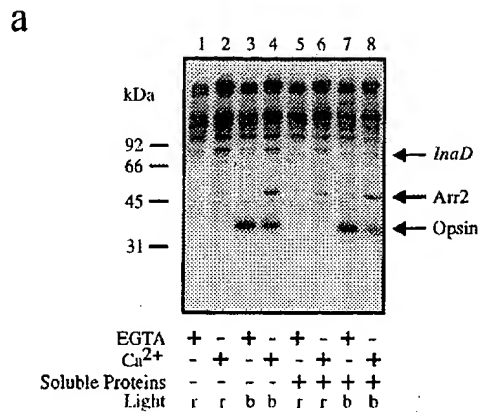

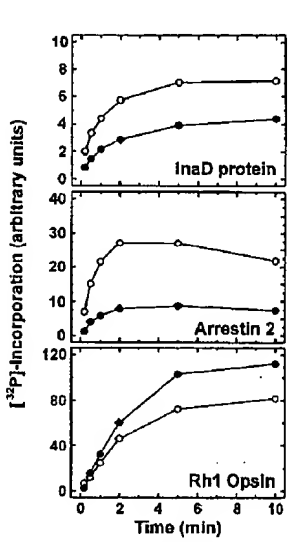

FIG. 6. **Ca^{2+}-dependent phosphorylation of the *InaD* protein.** *a*, purified photoreceptor membranes of 10 *Calliphora* retinae were phosphorylated in the presence of 2 mM EGTA (*lanes 1, 3, 5,* and *7*) or 60 μM calculated free Ca^{2+} (*lanes 2, 4, 6,* and *8*). In lanes 5–8 the membranes were reconstituted with a soluble extract obtained from six *Calliphora* retinae. Before starting phosphorylation by adding 2 mM ATP, samples were either kept under dim red light (*r, lanes 1, 2, 5,* and *6*) or illuminated with blue light for 2 min in order to convert 70% rhodopsin to metarhodopsin (*panel b, lanes 3, 4, 7,* and *8*). The phosphorylation reactions were carried out for 5 min in the dark. Migration of molecular weight standards is indicated on the *right*; *arrows* on the *left* show the position of the *InaD* protein (*InaD*), arrestin 2 (*Arr2*), and opsin. *b*, time course for the incorporation of radioactive phosphate into the *InaD* protein. For comparison, time courses of phosphorylation of arrestin 2 and opsin are shown. Phosphorylation reactions were performed in the absence (●), or presence (○) of Ca^{2+} as described in *panel a* for *lanes 3* and *4*, respectively. At the indicated times, the reactions were terminated by adding 5 × SDS-PAGE buffer. All samples were subjected to SDS-PAGE as described under "Experimental Procedures," and protein phosphorylation was detected by autoradiography or quantified by using a phosphor imager.

tein is assumed to be a Ca^{2+}-dependent protein kinase, we tested the effect of Ca^{2+} on the phosphorylation of the *InaD* protein and compared its phosphorylation with phosphorylation of rhodopsin and arrestin, which has been studied previously (14–17) (Fig. 6). Lowering of internal Ca^{2+} by the addition of 2 mM EGTA to the phosphorylation assay significantly reduced the incorporation of radioactive phosphate into the *InaD* protein as compared with standard phosphorylation assays performed at a calculated free Ca^{2+} concentration of 60 μM. Under these conditions, the phosphorylation of two other proteins involved in signal transduction is affected by lowering the free Ca^{2+} concentration. First, the amount of phosphorylated arrestin 2 associated with the rhabdomeral photoreceptor membrane is decreased. This finding is consistent with earlier reports indicating that arrestin 2 is phosphorylated by a Ca^{2+}-calmodulin-dependent protein kinase (17). Secondly, the phosphorylation of rhodopsin is affected by calcium concentration. There the amount of radioactive phosphate attached to metarhodopsin is reduced in the presence of Ca^{2+}, presumably due to dephosphorylation by a Ca^{2+}-dependent rhodopsin phosphatase (27, 28). We also investigated whether the light conditions to which the photoreceptor membranes were subjected before the reaction was started, might affect the incorporation of phosphate into the *InaD* protein. Under the *in vitro* conditions used here, the already intensively studied light activation of

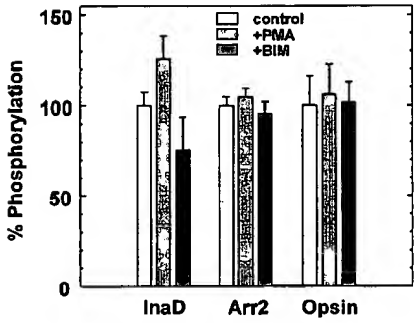

FIG. 7. **Effect of phorbolester and the protein kinase C inhibitor bisindolylmaleimide I on the phosphorylation of the *InaD* protein.** Phosphorylation of blue light-illuminated photoreceptor membranes was carried out under standard conditions (*control*), in the presence of 1 μM phorbol 12-myristate 13-acetate (*PMA*), and in the presence of 0.2 μM bisindolylmaleimide I (*BIM*). Samples were subjected to SDS-PAGE, and phosphorylation of the *InaD* protein (*InaD*), arrestin 2 (*Arr2*), and opsin was quantified using a phosphor imager. Data represent mean ± S.E. of four separate experiments. Statistical analysis using Student's *t* test shows that the effects of PMA and BIM on the phosphorylation of the *InaD* protein are significant (PMA-treated *versus* control: $t = -2.56$, $p = 0.042$; BIM-treated *versus* control: $t = 2.72$, $p = 0.034$). Phosphate incorporation into arrestin 2 and opsin shows no significant differences upon PMA or BIM treatment.

rhodopsin phosphorylation (14, 15) was reproduced, but light dependence of *InaD* protein phosphorylation was not revealed (Fig. 6*a*, *lanes 1* and *2* and *lanes 3* and *4*). Thus, we can exclude the possibility that activated rhodopsin (metarhodopsin), present in the membranes, directly promotes (or suppresses) the phosphorylation of the *InaD* protein. Furthermore, the addition of soluble proteins did not enhance the incorporation of phosphate into the *InaD* protein, but rather suppressed its phosphorylation (Fig. 6*a*, *lanes 5–8*). This indicates (i) that the protein kinase that catalyzes *InaD* phosphorylation resides in the photoreceptive membrane, and (ii) that soluble cofactors are not required for *InaD* protein phosphorylation.

Time courses of the protein phosphorylation revealed similar phosphorylation kinetics for the *InaD* protein and for opsin with no further increase in net phosphate incorporation 10 min after the reactions were started (Fig. 6*b*). Arrestin 2 phosphorylation, described as the most rapid protein phosphorylation observed in *Drosophila* eyes (29), saturated 2 min after starting the reactions. The Ca^{2+} dependence of the phosphate incorporation into the *InaD* protein, arrestin 2, and metarhodopsin is evident throughout the entire phosphorylation time course, except in the initial phase of metarhodopsin phosphorylation (Fig. 6*b*). The Ca^{2+}-enhanced phosphorylation of the *InaD* gene product suggested that this reaction is catalyzed either by a protein kinase C or by a Ca^{2+}-calmodulin-dependent protein kinase. In order to discriminate whether the *InaD* protein is phosphorylated by a protein kinase C or a Ca^{2+}-calmodulin-dependent protein kinase, protein kinase C was hyperactivated using a phorbolester or specifically inhibited with bisindolylmaleimide I. As shown in Fig. 7, the addition of phorbol 12-myristate 13-acetate to the phosphorylation reaction enhances the phosphate incorporation into the *InaD* protein by 25%. In the presence of bisindolylmaleimide I *InaD* protein phosphorylation is reduced by 25%. These effects are statistically significant (see legend of Fig. 7), and they are comparable with those observed in studies with other photoreceptor membrane proteins, for example the protein kinase C-dependent phosphorylation of bovine rhodopsin (30). The protein kinase C activator and inhibitor used here had no significant effect on the phosphorylation of arrestin 2 and opsin (Fig. 7), indicating that the addition of the phorbolester or of bisindolylmaleimide I modulated specifically the phosphorylation of the *InaD* protein but did not generally enhance or quench the phosphorylation of rhabdomeral proteins.

DISCUSSION

This study describes the molecular and biochemical characterization of the *Calliphora InaD* protein. The experiments have been performed to understand the function of this protein in the deactivation of light-triggered responses of photoreceptor cells. Cumulative evidence suggests that the biochemical reactions involved in phototransduction are identical in *Drosophila* and *Calliphora*. The eyes of both species have the same morphological architecture, they contain photoreceptors with identical absorbance characteristics, and the photoreceptor cells respond to light stimuli in the same way. Biochemical studies show that identified proteins of the phototransduction pathway, including Rh1 opsin (31–33), arrestin 2 (17, 27, 34), and phospholipase C (35, 36), perform identical functions in both species. However, these functionally homologous proteins are less conserved than they are between photoreceptors currently used as model systems of vertebrate phototransduction, for instance bovine, rat, and mouse. These differences in the overall homology allow us to identify conserved regions as probable sites of functional importance within the protein.

The sequence alignment of the *Drosophila* and *Calliphora InaD* proteins (see Fig. 1) highlights the weakly, as well as the highly, conserved regions of the protein sequences. The N-terminal region (amino acids 1–14 of the *Drosophila* sequence) and the stretch between amino acids 106 and 183 show little if any sequence homology, suggesting that these regions are functionally less important and were, therefore, subject to extensive mutation during the evolution of both fly species.

Other sites of the *InaD* protein are well conserved. With respect to the phosphorylation of the *InaD* protein investigated in the present study it is particularly striking that five out of eight conserved potential protein kinase C phosphorylation sites (at positions 19, 194, 329, 330, and 553) reside within stretches of 10–16 amino acids that are identical in the *Drosophila* and *Calliphora InaD* protein.

Despite the fact that there are some poorly conserved regions in the *Drosophila* and *Calliphora InaD* protein, the overall biophysical characteristics (for example the isoelectric point at 8.6, the high abundance of acidic and basic amino acids, and the hydrophilicity profile of both proteins) are nearly identical. The apparent molecular mass of about 75 kDa of the *Calliphora InaD* protein, as estimated by SDS-PAGE, fits the molecular mass calculated from the sequence data (73.4 kDa). The discrepancy between the calculated and apparent molecular mass of the *Drosophila InaD* protein (80 and 90 kDa, respectively) reported by Shieh and Niemeyer (11) is not evident in *Calliphora*. Due to the hydrophilic nature of the *InaD* protein, it has been proposed that the *Drosophila InaD* gene product is not an integral membrane protein (11). Our results obtained with the *Calliphora* homolog of *InaD* are in agreement with this prediction.

In the present study we show that the *InaD* protein is associated with the rhabdomeral photoreceptor membrane, from which it is extracted by buffers of high ionic strength. The attachment to the photoreceptive membrane may be crucial for *InaD* function, because functional impairment of the *Drosophila InaD* mutant ($InaD^{P215}$; Ref. 10) results from a single point mutation in which a methionine (Met^{442}), located within a small stretch of hydrophobic amino acids, is replaced by lysine (11). In the *Calliphora InaD* protein leucine is present at the corresponding position, indicating that Met^{442} is not necessarily required for normal *InaD* function, and may be exchanged with another hydrophobic amino acid. Distortion of the hydrophobic character of the region by a highly polar amino acid, for

example lysine of $InaD^{P215}$, however, might lead to the mutant phenotype, because the Met^{442} to Lys mutation may render a soluble *InaD* protein that is nonfunctional. Alternatively, the nonpolar character of this region may be crucial for hydrophobic protein-protein interactions. A significant contribution to the hydrophilic character of the *InaD* protein results from a conserved stretch of lysine and glutamate residues (see *bars* in Fig. 1*b*). Interestingly, similar lysine/glutamate-rich clusters are found in the bovine and mouse rod photoreceptor cGMP-gated channels (37, 38). Analysis of the structure-function relationship of cGMP-gated channels has not yet established the function of this hydrophilic cluster.

The biochemical experiments of the present study were designed to investigate whether or not the function of the *InaD* gene product might be controlled by phosphorylation. The striking conservation of several putative protein kinase C phosphorylation sites between the *Drosophila* and *Calliphora InaD* sequence (Fig. 1), the localization of the *InaD* protein and the *inaC* encoded eye-PKC in the rhabdomeral photoreceptor membranes (Fig. 2 and Ref. 13), and, most importantly, the co-immunoprecipitation of the *InaD* protein and eye-PKC (Fig. 3) suggest that the *InaD* protein is a likely candidate for phosphorylation by eye-PKC. Moreover, *Drosophila InaD* and *inaC* mutants show a similar phenotype, which is characterized by a defect in photoreceptor deactivation and by abnormal light adaptation (1, 2, 11, 13, 39), indicating that the respective gene products are acting, or even interacting, in closely related steps of the transduction cascade. The phosphorylation studies presented here reveal that the *InaD* protein is a phosphoprotein (Figs. 4 and 5). The Ca^{2+}-dependence of the *InaD* protein phosphorylation (Fig. 6) and the findings that the incorporation of phosphate into the *InaD* protein is moderately enhanced in the presence of a phorbolester and quenched by the protein kinase C inhibitor bisindolylmaleimide (Fig. 7) are in line with the assumption that this phosphorylation is catalyzed by eye-PKC.

Despite this evidence, the data do not yet allow us to unequivocally rule out the possibility of phosphorylation of the *InaD* protein by other protein kinases. Ca^{2+}-dependent phosphorylation of arrestin 2, reported to result from a Ca^{2+}-calmodulin-dependent protein kinase (17), is observed in parallel to the Ca^{2+}-dependent phosphorylation of the *InaD* protein, indicating that the corresponding protein kinase is present in the membrane preparation used in the assays. Also, Matsumoto and colleagues (17, 40, 41) reported on the phosphorylation of an 80-kDa protein present in the photoreceptor cell layer of *Drosophila* eyes. The molecular mass of this phosphoprotein suggests that it might represent the *Drosophila InaD* protein. However, the phosphorylation of this *Drosophila* 80-kDa protein was shown to be activated by cAMP but not by calcium (17). At least the *Calliphora InaD* protein lacks consensus sites for phosphorylation by a cAMP-dependent protein kinase. In dark-adapted *Drosophila* eyes, this 80-kDa protein is in the nonphosphorylated state, but it rapidly (within 3 s) becomes phosphorylated when the flies are exposed to a 1-ms light flash (41). Furthermore, the light-dependent phosphorylation of this protein is not observed in *Drosophila norpA* mutants (40), indicating that it depends on the activation of the phototransduction cascade and occurs downstream of the *norpA*-encoded phospholipase C.

Phosphorylation by protein kinase C is shown to be involved in the desensitization of a number of vertebrate G-protein-mediated transduction cascades, *e.g.* vertebrate phototransduction (30, 42) and β-adrenergic receptor signaling (43). There desensitization is achieved by a protein kinase C-dependent phosphorylation of the respective receptor (rhodopsin or β-adrenergic receptor), which in contrary to the phosphorylation by rhodopsin kinase or β-adrenergic receptor kinase, occurs in the activated and the nonactivated state of the receptor. Protein kinase C-mediated phosphorylation was shown to uncouple the receptor from its G-protein (44), thereby terminating the signal response. The proposed deactivation of the visual response via phosphorylation of the *InaD* protein by eye-PKC would act at a different site of the transduction cascade.

Towards a model for the Ca^{2+}-dependent response inactivation in fly photoreceptor cells, we propose that the *InaD* protein is modulated via phosphorylation by eye-PKC, which itself should be activated by the transient rise of the intracellular Ca^{2+} concentration upon visual excitation. Phosphorylated *InaD* protein in turn may be a subunit of, or act on, a third protein, *e.g.* an ion channel, in order to regulate Ca^{2+} influx into the cytosol. In this respect it is important to note that the *trp* protein, which is proposed to represent a novel Ca^{2+} channel responsible for light-dependent inositol trisphosphate-mediated Ca^{2+} entry (6, 7), co-immunoprecipitates with the *InaD* protein. Alternatively, the activated *InaD* protein could be part of a feedback control mechanism that acts on upstream members of the transduction cascade. One of these may be the *norpA*-encoded phospholipase C (11). Our finding that key proteins of the phototransduction cascade investigated here co-immunoprecipitate with the *InaD* protein may indicate that proteins that provide a control mechanism of visual excitation are associated into a functional protein complex.

In conclusion, we have for the first time provided evidence that the *Calliphora* homolog of the *InaD* protein is phosphorylated by the *inaC*-encoded eye-PKC. *InaD* protein phosphorylation may be part of the mechanism that regulates the deactivation of the light response in invertebrate photoreceptors, in a way that is distinct from the protein kinase C-mediated desensitization of vertebrate phototransduction or β-adrenergic receptor signaling. However, a similar mechanism may operate in other vertebrate and invertebrate signaling pathways in which *trp* homologs are used as part of a store-operated Ca^{2+} entry (45).

Acknowledgments—We thank R. Shortridge and J. B. Hurley for providing anti-*norpA* and anti-$G_{\beta e}$ antibodies. We are grateful to G. Gerdon and M. Bähner for expert technical assistance in immunoscreening cDNA libraries and in sequencing the *InaD* clone and to T. P. Williams for helpful comments on the manuscript.

REFERENCES

1. Ranganathan, R., Harris, G. L., Stevens, C. F., and Zuker, C. S. (1991) *Nature* **345**, 230–232
2. Hardie, R. C. (1991) *Proc. R. Soc. London Ser. B* **245**, 203–210
3. Sandler, C., and Kirschfeld, K. (1991) *J. Comp. Physiol. A* **169**, 299–311
4. Peretz, A., Sandler, C., Kirschfeld, K., Hardie, R. C., and Minke, B. (1994) *J. Gen. Physiol.* **104**, 1057–1077
5. Mojet, M. H. (1993) *J. Comp. Physiol. A* **173**, 335–346
6. Hardie, R. C., and Minke, B. (1993) *Trends Neurosci.* **16**, 371–376
7. Hardie, R. C., and Minke, B. (1992) *Neuron* **8**, 643–651
8. Wong, F., Schaefer, E. L., Roop, B. C., LaMendola, J. N., Johnson-Seaton, D., and Shao, D. (1989) *Neuron* **2**, 81–94
9. Montell, C., and Rubin, G. M. (1989) *Neuron* **2**, 1313–1323
10. Pak, W. L. (1979) in *Neurogenetics: Genetic Approaches to the Nervous System* (Breakfield, X. O., ed) pp. 67–99, Elsevier, New York
11. Shieh, B.-H., and Niemeyer, B. (1995) *Neuron* **14**, 201–210
12. Schaeffer, E., Smith, D., Mardon, G., Quinn, W., and Zuker, C. (1989) *Cell* **57**, 403–412
13. Smith, D. P., Ranganathan, Hardie, R. W., Marx, J., Tsuchida, T., and Zuker, C. S. (1991) *Science* **254**, 1478–1484
14. Paulsen, R., and Bentrop, J. (1984) *J. Comp. Physiol. A* **155**, 39–45
15. Bentrop, J., and Paulsen, R. (1986) *Eur. J. Biochem.* **161**, 61–67
16. Komori, N., Usukura, J., Kurien, B., Shichi, H., and Matsumoto, H. (1994) *Insect Biochem. Mol. Biol.* **24**, 607–617
17. Yamada, T., Takeuchi, Y., Komori, N., Kobayashi, H., Sakai, Y., Hotta, Y., and Matsumoto, H. (1990) *Science* **248**, 483–486
18. Paulsen, R. (1984) *J. Comp. Physiol. A* **155**, 47–55
19. Harlow, E., and Lane, D. (1988) *Antibodies: A Laboratory Manual*, Cold Spring Harbor Laboratory, Cold Spring Harbor, New York
20. Zhu, L., McKay, R. R., Shortridge, R. D., (1993) *J. Biol. Chem.* **268**, 15994–16001
21. Dolph, P. J., Man-Son-Hing, H., Yarfitz, S., Colley, N. J., Running Deer, J.,

Spencer, M., Hurley, J. B., and Zuker, C. S. (1994) *Nature* **370,** 59–61
22. Sambrook, J., Fritsch, E. F., and Maniatis, T. (1989) *Molecular Cloning: A Laboratory Manual*, 2nd Ed., Cold Spring Harbor Laboratory, Cold Spring Harbor, New York
23. Sanger, F., Nicklen, S., and Coulson, A. R. (1977) *Proc. Natl. Acad. Sci. U. S. A.* **74,** 5463–5467
24. Laemmli, U. K. (1970) *Nature* **227,** 680–685
25. Fabiato, A. (1988) *Methods Encymoi.* **157,** 378–416
26. Cavener, D. R. (1987) *Nucleic Acids Res.* **15,** 1353–1361
27. Plangger, A., Malicki, D., Whitney, M., and Paulsen, R. (1994) *J. Biol. Chem.* **269,** 26969–26975
28. Byk, T., Bar-Yaacov, M., Doza, Y. N., Minke, B., and Selinger, Z. (1993) *Proc. Natl. Acad. Sci. U. S. A.* **90,** 1907–1911
29. Matsumoto, H., Kurien, B. T., Takagi, Y., Kahn, E. S., Kinumi, T., Komori, N., Yamada, T., Hayashi, F., Isono, K., Pak, W. L., Jackson, K. W., and Tobin, S. L. (1994) *Neuron* **12,** 997-1010
30. Newton, A. C., and Williams, D. S. (1993) *J. Biol. Chem.* **268,** 18181–18186
31. Zuker, C. S., Cowman, A. F., and Rubin, G. M. (1985) *Celi* **40,** 851–858
32. O'Tousa, J. E., Baehr, W., Martin, R. L., Hirsch, J., Pak, W. L., and Applebury, M. L. (1985) *Celi* **40,** 839–850
33. Huber, A., Smith, D. P., Zuker, C. S., and Paulsen, R. (1990) *J. Biol. Chem.* **265,** 17906–17910
34. Hyde, D. R., Mecklenburg, K. L., Pollock, J. A., Vithelic, T. S., and Benzer, S. (1990) *Proc. Natl. Acad. Sci. U. S. A.* **87,** 1008–1012
35. Bloomquist, B. T., Shortridge, R. D., Schneuwly, S., Perdew, M., Montell, C., Steller, H., Rubin, G. M., and Pak, W. L. (1988) *Celi* **54,** 723–733
36. McKay, R. R., Miller, K., Weckström, M., Torkkeli, P., Järviletho, M., and Shortridge, R. D. (1994) *J. Neurogenetics* **9,** 177–187
37. Kaupp, U. B., Niidome, T., Tanabe, T., Terada, S., Bönigk, W., Stühmer, W., Cook, N. J., Kangawa, K., Matsuo, H., Hirose, T., Miyata, T., and Numa, S. (1989) *Nature* **342,** 762–766
38. Ludwig, J., Margalit, T., Eismann, E., Lancet, D., and Kaupp, U. B. (1990) *FEBS Lett.* **270,** 24–29
39. Hardie, R. C., Peretz, A., Suss-Toby, E., Rom-Glas, A., Bishop, S. A., Selinger, Z., and Minke, B. (1993) *Nature* **363,** 634–637
40. Matsumoto, H., O'Tousa, J. E., and Pak, W. L. (1982) *Science* **217,** 839–841
41. Matsumoto, H., and Pak, W. L. (1984) *Science* **223,** 184–186
42. Greene, N. M., Williams, D. S., and Newton, A. C. (1995) *J. Biol. Chem.* **270,** 6710–6717
43. Picher, J., Lohse, M. J., Codina, J., Caron, M. G., and Lefkowitz, R. J. (1992) *Biochemistry* **31,** 3193–3197
44. Kelleher, D. J., and Johnson, G. L. (1986) *J. Biol. Chem.* **261,** 4749–4757
45. Wes, P. D., Chevesich, J., Jeromin, A., Rosenberg, C., Stetten, G., and Montell, C. (1995) *Proc. Natl. Acad. Sci. U. S. A.* **92,** 9652–9656
46. Kyte, J., and Doolittle, R. F. (1982) *J. Mol. Biol.* **157,** 105–132

Proc. Natl. Acad. Sci. USA
Vol. 91, pp. 9818–9822, October 1994
Biochemistry

Cloning and characterization of hdlg: The human homologue of the *Drosophila* discs large tumor suppressor binds to protein 4.1

(PSD-95/p55/guanylate kinase/cell–cell contact)

ROBERT A. LUE*, SHIRIN M. MARFATIA†, DANIEL BRANTON*‡, AND ATHAR H. CHISHTI†

*Department of Molecular and Cellular Biology, Harvard University, 16 Divinity Avenue, Cambridge, MA 02138; and †Department of Biomedical Research, St. Elizabeth's Medical Center, Tufts University School of Medicine, Boston, MA 02135

Contributed by Daniel Branton, June 28, 1994

ABSTRACT **The *Drosophila* discs large tumor suppressor protein, dlg, has been shown to regulate the growth of imaginal discs during embryogenesis [Woods, D. F. & Bryant, P. J. (1991) *Cell* 66, 451–464]. We cloned and sequenced the complete cDNA for a human B-lymphocyte 100-kDa protein that shares 60% amino acid identity with dlg. This human homologue of *Drosophila* discs large (hdlg) contains a C-terminal domain homologous to the known guanylate kinases, a src homology 3 region motif, and three dlg homology repeats. Two nonhomologous domains that can contain in-frame insertions result in at least four alternatively spliced isoforms of hdlg. Several hdlg RNA transcripts are widely distributed in human and murine tissues, and the protein is localized to regions of cell–cell contact. Protein 4.1, the defining member of a family that includes talin and merlin/schwannomin, has the same cellular localization as hdlg, and two sites within hdlg associate *in vitro* with the 30-kDa N-terminal domain of protein 4.1.**

Recessive lesions in seven *Drosophila* genes that have been described as tumor suppressors lead to overgrowth of the imaginal discs. In the lethal (1) discs large 1 (*dlg*) locus, germ-line mutations result in imaginal disc neoplasia and a prolonged larval period followed by death (1). The amino acid sequence of dlg includes several conserved domains: three repetitive sequence motifs containing the sequence GLGF, which have been called dlg homology repeat (DHR) segments, a src homology 3 region (SH3) motif, and a domain that is homologous to the known guanylate kinases (2) (see Fig. 1*A*). These domains, and their organization relative to one another, are conserved across an emerging family of proteins, which include the rat synaptic protein PSD-95, or SAP90 (3, 4), the tight junction proteins ZO-1 and ZO-2 (5–7), and human erythroid p55 (8). We have cloned several isoforms of the human homologue of *Drosophila* dlg (hdlg) from B lymphocytes and present here their sequence features[§] and the general tissue distribution of their RNA transcripts. We also show that both hdlg and protein 4.1 immunolocalize to regions of cell–cell contact and provide *in vitro* evidence for the specific association of the 30-kDa domain of protein 4.1 with two sites on hdlg.

MATERIALS AND METHODS

PCR Screen for hdlg cDNAs. Total RNA was isolated from BM14 B-lymphoblastoid cells using the guanidinium thiocyanate method (9). Single-stranded cDNA was reverse transcribed from 5 μg of RNA after priming with a $(dT)_{17}$+adapter primer as described (10). Each single-stranded cDNA stock was then diluted 100-fold and used in subsequent PCR reactions. We synthesized degenerate primers complementary to four 5-aa stretches flanking two regions of homology between dlg and PSD-95: GLGFN and WWQAR (region A) and GGTDN and NQHIP (region B). Primer sequences were based on the mammalian codon preference: region A primers RPT-1 (sense) GG(N)CT(B)G-G(N)TT(Y)AA(Y)A and RPT-2 (antisense) (N)CG(N)G-C(Y)TGCCACCA; region B primers RPT-3 (sense) G(N)G-G(N)AC(N)GA(Y)AA(Y)CC and RPT-4 (antisense), G(N)G-G(D)AT(R)TG(Y)TG(R)TT (N = G, A, T, or C; B = G, T, or C; Y = T or C; R = G or A; D = G, A, or T). PCR reactions were carried out at low stringency, and products of the predicted size were resolved on agarose gels, excised, and purified before subcloning into a PCR II TA Cloning vector (Invitrogen). The resultant cDNA inserts were sequenced and compared with the analogous region of *dlg*. Out of 24 clones sequenced, 18 showing >65% amino acid identity with dlg were judged positive for the hdlg sequence.

The remaining 5′ and 3′ portions of the hdlg cDNA were cloned using a modified rapid amplification of cDNA ends protocol based on two successive rounds of PCR amplification using nested primers. In the case of the 3′ end, the first round of PCR amplification used the B-lymphocyte $(dT)_{17}$+adapter-primed single-stranded cDNA, probed with primers specific for hdlg and the adapter. The weakly amplified products were resolved on a 3% low-melting-point agarose gel, and the region corresponding to 1–2 kb was excised for use in the secondary PCR reaction with a different pair of nested primers. Products of the secondary PCR were isolated, subcloned, and sequenced as before. All 12 clones sequenced were found to contain the 3′ stop codon of hdlg.

To increase the likelihood of cloning the 5′ portion of hdlg, a selective cDNA minilibrary was reverse transcribed from BM14 RNA primed with a mixture of hdlg-specific oligonucleotides. Replacement synthesis of the second strand was performed as described (11), and the resultant double-stranded cDNA pool was ligated into pBS-SK (Stratagene). The minilibrary was used as the template for two successive rounds of PCR amplification with nested primers as described above. Out of 18 clones sequenced, 5 were found to contain the initiating methionine of hdlg. Analysis of several 5′ and 3′ partial clones revealed sequence insertions in each. Three different insertions, I1, I2, and I3, were isolated.

Northern Blots. Total RNA was isolated from the BM14 B-lymphocyte cell line by the guanidinium thiocyanate method (9), and Northern blots were prepared by standard methods (10). Northern blots derived from multiple human and murine tissues containing 2 μg of poly(A)$^+$ RNA per lane were obtained from Clontech. The blots were probed with a 1150-bp cDNA fragment of hdlg (bases 504–1654) that had been nick-translated with [^{32}P]dCTP (10).

The publication costs of this article were defrayed in part by page charge payment. This article must therefore be hereby marked "*advertisement*" in accordance with 18 U.S.C. §1734 solely to indicate this fact.

Abbreviations: hdlg, human homologue of *Drosophila* dlg; GST, glutathione *S*-transferase; GUK, guanylate kinase; SH3, src homology 3 region; DHR, dlg homology repeat.

‡To whom reprint requests should be addressed.

§The sequences reported in this paper have been deposited in the GenBank data base (accession nos. U13896 and U13897).

Expression of Recombinant hdlg. Plasmid constructs were made that expressed the following as glutathione *S*-transferase (GST) fusion proteins: the entire coding region (accession no. U13897) of hdlg (GST–FL), the N-terminal domain from amino acid 1 to 223 (GST–NT), the three DHR segments from amino acid 201 to 584 (GST–DHR), and the SH3 and guanylate kinase (GUK) domains together from amino acid 584 to 904 (GST–SH3/GUK). The appropriate sequences were PCR amplified from BM14 single-stranded cDNA, and the products were ligated into pGEX-2t (Pharmacia) in-frame for expression as GST fusion proteins in *Escherichia coli*. All constructs were sequenced and produced soluble fusion proteins of the expected sizes. Full-length hdlg constructs bearing I3 alone (GST–FL^{I3}) and SH3/GUK constructs with either I2 (GST–SH3/GUK^{I2}) or I3 (GST–SH3/GUK^{I3}) were isolated.

Generation of Antibodies and Immunofluorescence Microscopy. The hdlg moiety containing all three DHR segments was cleaved from the purified GST–DHR fusion protein using thrombin (12). After further purification on an anion-exchange column, the antigen was used to produce rabbit antibodies as described (13). Anti-hdlg serum (no. 742) was used at a 1:100 dilution to immunostain methanol-fixed MCF-7 human breast carcinoma cells grown on glass coverslips. Cells were also probed with anti-protein 4.1 affinity-purified IgG (no. 14) as described (14). Probes were visualized using a goat anti-rabbit secondary antibody conjugated to fluorescein isothiocyanate and viewed on a Bio-Rad model MRC600 confocal microscope.

Binding Assays with Protein 4.1. Binding assays were performed using 2 μg of GST fusion protein immobilized on 15 μl of packed glutathione beads. In all cases, beads with immobilized protein were incubated with radiolabeled protein 4.1 or its 30-kDa domain in binding buffer [5.0 mM sodium phosphate (pH 7.6), 1.0 mM 2-mercaptoethanol, 0.5 mM EDTA, 120 mM KCl, 0.02% sodium azide, and bovine serum albumin at 1.0 mg/ml; total volume, 50–500 μl]. After incubation for 1–2 hr at 4°C with gentle mixing, the beads were washed five times in 1.5 ml of binding buffer, aspirated to dryness, and either placed in a γ counter (for ^{125}I-labeled 30-kDa domain; triplicate samples) or the bound protein was released in 30 μl of SDS sample buffer for SDS/PAGE followed by autoradiography (for ^{14}C-labeled protein 4.1).

RESULTS

Cloning of hdlg. Since it was unclear whether the human homologue of dlg (hdlg) would be an alternatively spliced form of the p55 transcript or a product of a second distinct gene, we first probed with DNA primers complementary to a conserved region that included the DHR1 segment shared by all of the family members. Out of 24 clones that were sequenced, none corresponded to alternatively spliced transcripts that could account for a dlg-like protein. We then probed by PCR for other conserved regions of dlg not shared by p55: region A (Fig. 1*A*) spanned the middle of DHR3 to the middle of the SH3 motif; region B spanned DHR1 and DHR2. The upstream sense oligonucleotide, which defined the boundary of region A, and the oligonucleotides that defined both boundaries of region B encoded amino acid sequences shared only by dlg and PSD-95/SAP90.

The PCR screen for regions A and B yielded products of the expected sizes. The predicted amino acid sequence of both PCR products was 65% identical to that of the analogous regions in dlg. We then selectively reverse transcribed cDNA from BM14 RNA primed with oligonucleotides specific for the hdlg partial sequence and were able to clone the remainder of the cDNA using a modified rapid amplification of cDNA ends protocol described in *Materials and Methods*.

The hdlg clones were 60% identical to dlg and 70% identical to rat PSD-95/SAP90 on the protein level. The complete sequences have been deposited in GenBank (accession nos. U13896 and U13897). The domain organization characteristic of the other family members was also conserved, with three DHR segments in the N-terminal half of the protein, a central SH3 motif, and a C-terminal GUK domain (Fig. 1*A*). The three DHR segments were between 40% and 53% identical to each other and up to 90% identical to the analogous segments in PSD-95/SAP90. The SH3 motif was most similar to that of dlg with 70% amino acid identity, followed by that of PSD-95/SAP90 and crk. The GUK domain was 40% identical to the entire protein sequence of yeast GUK and 80% identical to the analogous domain in dlg and PSD-95/SAP90. The hdlg GUK domain, like that of dlg and PSD-95/SAP90, had a 3-aa deletion in a glycine-rich motif that is similar to the predicted ATP-binding site of yeast guanylate kinase (15).

Two regions of the hdlg sequence not found in the other family members might represent novel functional domains: a charged, proline-rich 190-aa N-terminal domain (Fig. 1*B*) and a 40-aa internal domain between the SH3 and GUK domains (Fig. 1*C*). When the 5′ and 3′ portions of the hdlg cDNA were PCR amplified from our cDNA minilibrary, both classes of products ran as doublets on agarose gels. Sequence analysis of these PCR products revealed possible insertions in each of the two domains. In the N-terminal domain, either a 99-base insertion (I1) or no insertion occurred after base number 483 (Fig. 1*B*), whereas in the 3′ region either a 36-base (I2) or 102-base (I3) insertion occurred after base 1905 (Fig. 1*C*). The insertions were in-frame, and all of the four possible combinations of 5′ and 3′ insertions were represented among our clones. The I1 insertion in the N-terminal domain encoded a sequence that is particularly proline-rich (10 out of 33) with several tandem sequences similar to the recently derived SH3-binding consensus (16, 17). The I2 insertion was not homologous to other known sequences, while the I3 insertion was 38% identical to the region spanning amino acids 693–727 of dlg, which also lies between the SH3 and GUK domains.

Distribution of hdlg Protein and mRNA. hdlg protein and message were widely distributed in human and murine tissues. Rabbit serum raised against the DHR domain of hdlg, consisting of all three DHR segments, reacted strongly with several proteins around 100 kDa in size and weakly with three proteins between 29 and 42 kDa from human B cells, lung fibroblasts, and cervical epithelia and murine fibroblasts and T cells (Fig. 2). The weakly reactive smaller bands may be due to other proteins with conserved DHR segments or breakdown products of hdlg. No cross-reactivity was observed with erythroid p55.

Northern blots of mRNA isolated from several human tissues all revealed several closely spaced hdlg transcripts whose sizes ranged between 5 and 5.5 kb (Fig. 3). The close spacing of the hybridization signals was consistent with the presence of isoform-dependent sequence insertions. Northern blots of murine tissues revealed a similar pattern of hybridization for multiple isoforms (data not shown).

Immunolocalization of hdlg Protein. The known localization of dlg at septate junctions (2) together with our recent observations that erythroid p55 binds *in vitro* to protein 4.1, a membrane-associated protein (19), raised the possibility that hdlg might be localized to membranes and regions of cell–cell contact. Indeed, the polyclonal antibodies raised against the DHR domain of hdlg specifically stained regions of cell–cell contact in human MCF-7 cells (Fig. 4*A*), and similar membrane associated staining was observed with an antibody to erythroid protein 4.1 (Fig. 4*B*). In both cases, no staining was observed with preimmune serum or anti-hdlg serum preincubated with an excess of hdlg (Fig. 4*C*).

hdlg Binds to Protein 4.1. To determine if the colocalization of hdlg and protein 4.1 represented a direct interaction between the two proteins, various GST–hdlg fusion proteins immobilized on glutathione-agarose beads were incubated

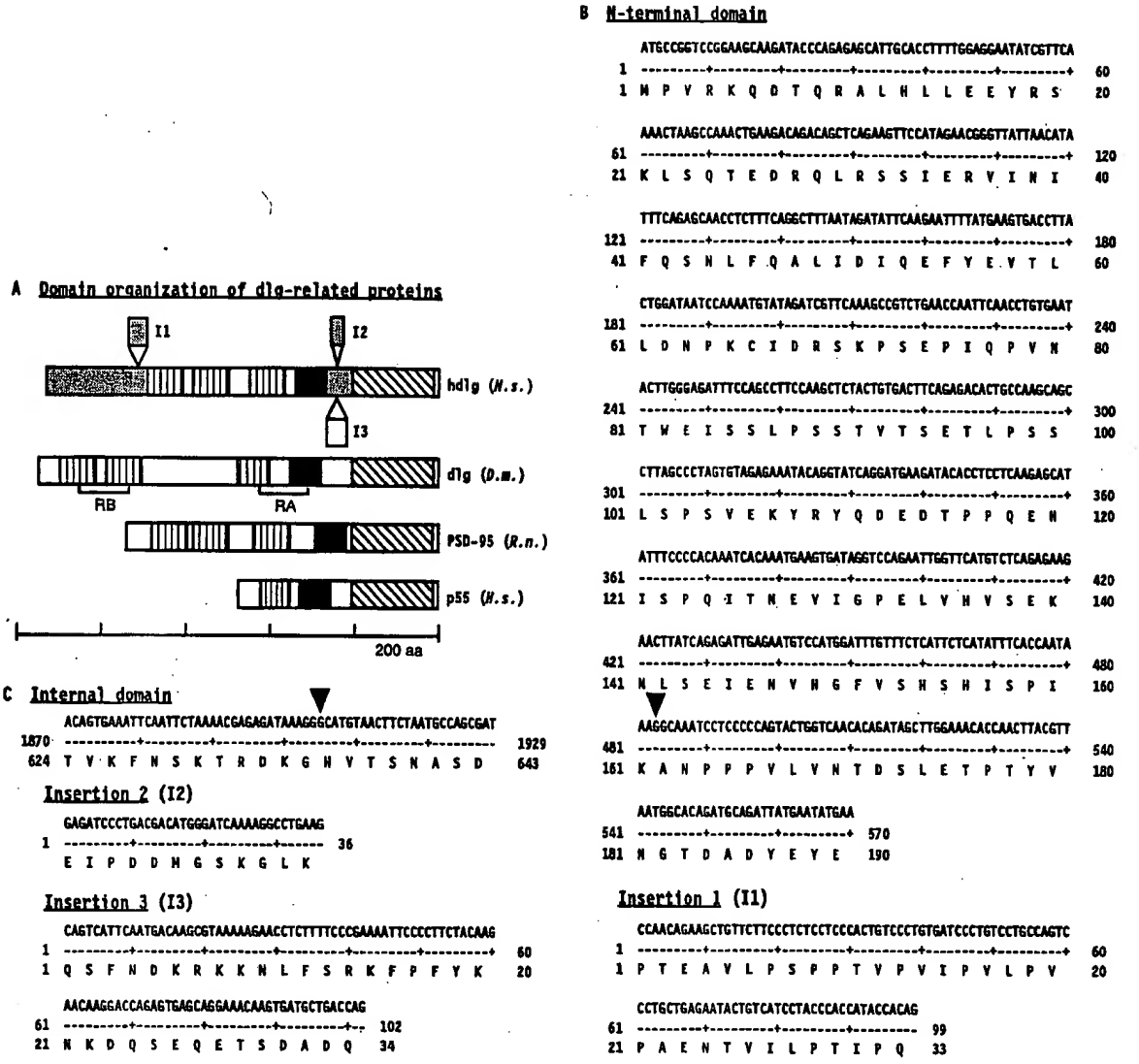

FIG. 1. Sequence domains of hdlg. (*A*) Comparative domain organization of dlg-related proteins. Only the most closely related proteins are shown. The diagonally hatched boxes represent the GUK domains; black boxes, SH3 motifs; vertically striped boxes, DHR segments; and gray boxes, domains and insertions found only in hdlg. The two regions of homology (RA and RB) that were used to design degenerate PCR probes are indicated below dlg. (*B* and *C*) Nucleotide sequence and deduced amino acid sequence of the N-terminal and internal domains found only in hdlg. A black triangle denotes the nucleotide after which at least one isoform insertion has been found to occur. The sequences of the isoform insertion(s) are also given below the domain in which they occur. *H.s., Homo sapiens; D.m., Drosophila melanogaster; R.n., Rattus norvegicus.*

with ^{14}C-labeled protein 4.1 and then sedimented. Both lymphocyte protein 4.1 as well as a 30-kDa labeled breakdown product bound to the beads in an hdlg-dependent manner (Fig. 5, lanes 1–3). Binding to protein 4.1 was mapped to two sites on hdlg: the DHR domain containing all three repeat segments (Fig. 5, lane 4) and the I3 insertion found between the SH3 and GUK domains in a subset of hdlg isoforms (Fig. 5, lanes 5 and 6). Because the N-terminal 30-kDa domain is a well-characterized α-chymotrypsin digestion product of protein 4.1 (21), we confirmed that this domain contains the predominant site that interacts with hdlg at both sites (Table 1). This result is also consistent with our

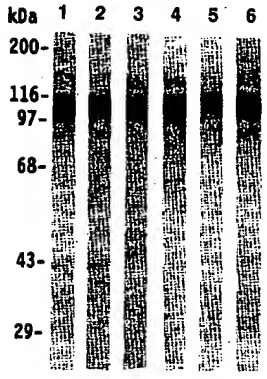

FIG. 2. Western blots of whole-cell lysates probed with anti-hdlg antibodies. Lanes: 1, human BM14 B lymphocytes; 2, HeLa cells; 3, HT29 cells; 4, W138 cells; 5, NIH 3T3 cells; 6, murine T lymphocytes. Whole-cell lysates were resolved by SDS/PAGE, blotted to nitrocellulose, and probed with anti-hdlg polyclonal serum diluted 1:1000 (18). Immunoreactive bands were visualized as described (18) after incubation with goat anti-rabbit IgG conjugated to alkaline phosphatase.

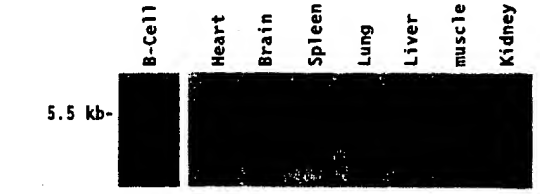

FIG. 3. Northern blots of human mRNA probed with the hdlg cDNA sequence. The tissue source of the blotted RNA is indicated above each lane.

FIG. 4. Immunofluorescence localization of hdlg and protein 4.1 in human MCF-7 cells. Cells were stained with anti-hdlg rabbit immune sera (*A*), with anti-protein 4.1 affinity-purified IgG (*B*), or with anti-hdlg rabbit immune sera preabsorbed against hdlg protein (*C*).

recent finding that the 30-kDa domain of protein 4.1 binds to erythroid p55 within a 38-aa segment flanked by the SH3 and GUK domains (unpublished results).

DISCUSSION

Our results identify the human homologue of *Drosophila* dlg. The hdlg sequence shows that it is a gene distinct from that of p55, and its inclusion in the family of dlg-related proteins provides further evidence that there are two classes of family members: the larger homologues, including hdlg, PSD-95/SAP90, and ZO-1, and the smaller homologues, such as p55. Both hdlg and p55 (24) transcripts are also widely distributed in human and mouse tissues, indicating that large and small dlg-related proteins coexist in many cell types.

All dlg-related proteins share an ≈190-aa domain homologous to the entire length of the yeast GUK enzyme (25), but the large anion pit that is predicted to be the ATP-binding site of GUK (15) is disrupted by a 3-aa deletion in hdlg and the other large family members (26). While the effect of this deletion on the putative enzymatic activity of the dlg homologues has yet to be demonstrated, the GUK domain may not be an active GUK but, instead, a regulatory site that binds guanine nucleotides, as do other G proteins.

A distinctive feature of both hdlg and ZO-1 is the presence of both an SH3 motif and a proline-rich domain in the same protein. The I1 insertion following base 483 encodes a polyproline domain that contains sequences similar to the SH3-binding consensus motifs derived from 3BP-1 (16), mSos1 (27), and dynamin (28) (Fig. 6*A*). Based on the differing specificities observed with the three SH3-binding proteins, the I1 sequence can be divided into several tandem SH3-binding motifs that may bind to more than one class of SH3 domains in a regulated fashion. Furthermore, the $(PXX)_n$ spacing of proline residues is consistent with the formation of an extended polyproline II helix (29), a structure that has been shown to interact with the conserved hydrophobic groove common to the known SH3 structures (30).

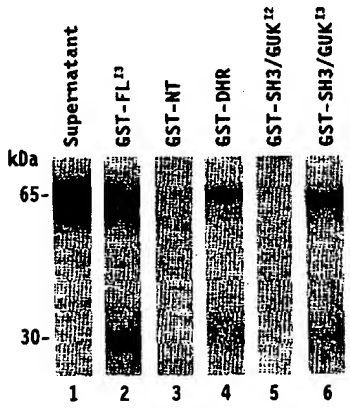

FIG. 5. Association of expressed ^{14}C-labeled protein 4.1 with GST–hdlg fusion proteins immobilized on beads. Autoradiograms of the labeled protein 4.1 in the supernatant (lane 1) and associated with the bead pellet (lanes 2–6) are shown. The immobilized proteins are indicated above each lane. The ^{14}C-labeled protein 4.1 was prepared as follows: A partial protein 4.1 cDNA sequence spanning the second downstream initiating methionine codon to the 3′ end of the reported spectrin binding domain (20) was PCR amplified from the BM14 B-lymphocyte single-stranded cDNA pool described earlier. The PCR product was subcloned into N8, an SP6 eukaryotic expression vector, and expressed in a coupled transcription/translation system (TNT coupled reticulocyte lysate system; Promega) supplemented with [^{14}C]leucine according to the manufacturer's directions.

The hdlg-binding site on protein 4.1 is located within the N-terminal 30-kDa domain, which is conserved in other protein 4.1 family members including talin (31), ezrin (32), the human protein tyrosine phosphatase MEG (33) and the NF2 gene product merlin/schwannomin (34, 35). Protein 4.1 in human erythrocytes links the spectrin network to the membrane via glycophorin C and has been immunolocalized to adherens junctions in epithelial cells (36). Talin is localized at sites of focal adhesion in fibroblasts and at cell–cell contact regions in lymphocytes, perhaps via association with integrins (37, 38). Ezrin, moesin, and radixin have also been immunolocalized to cell–cell adherens junctions and focal adhesion plaques (39). Given that hdlg and protein 4.1 exhibit the same staining pattern at regions of cell–cell contact in MCF-7 cells, hdlg's submembrane localization may be the consequence of interactions with either protein 4.1 or another member of the 4.1 family. Indeed, *Drosophila* protein 4.1 has recently been localized to septate junctions (40) precisely where dlg is located (2), suggesting that the interaction between hdlg and protein 4.1 may be functionally relevant in both vertebrates and invertebrates.

All of the large dlg homologues known contain a DHR domain composed of three 90-aa repeats termed DHR segments. Several proteins contain single DHR segments in-

Table 1. Specific association of the 30-kDa domain of protein 4.1 with the DHR domain and I3 insertion of hdlg

Fusion protein	Bound 30-kDa domain of protein 4.1, cpm
GST–FL[I3]	1770 ± 19
GST–FL[I3] + protein 4.1	552 ± 49
GST–NT	269 ± 30
GST–DHR	1452 ± 49
GST–SH3/GUK[I2]	309 ± 36
GST–SH3/GUK[I3]	2115 ± 53

Each of the bead-immobilized fusion proteins was preincubated in buffer alone or buffer plus a 10-fold molar excess of protein 4.1, washed, and incubated with identical aliquots of the ^{125}I-labeled 30-kDa domain of protein 4.1 (see *Materials and Methods*). Each value represents the average of three assays ± SD. The ^{125}I-labeled 30-kDa domain was prepared from purified protein 4.1 (22), labeled with ^{125}I-Bolton–Hunter reagent (23), digested to completion with α-chymotrypsin (enzyme to substrate ratio of 1:25), and separated from other fragments on a DEAE-Sephacel column. SDS/PAGE followed by autoradiography showed that >95% of the label was in the 30-kDa domain.

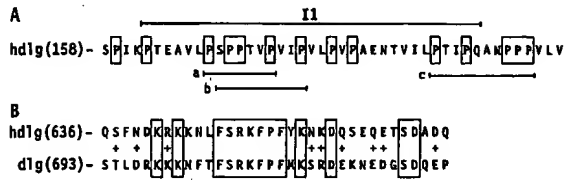

FIG. 6. (*A*) Sequence of the proline-rich region formed by the I1 insertion in the N-terminal domain of hdlg. Proline residues are boxed, and the boundaries of the I1 insertion are bracketed above. Regions that match the proline arrangement found in the SH3-binding motifs of dynamin (a), mSos (b), and 3BP-1 (c) are bracketed below the protein sequence. (*B*) Sequence alignment of the I3 insertion with the analogous region of *Drosophila* dlg. Amino acid identities are boxed, and conservative substitutions are indicated by "+." The first residue position is indicated in parentheses.

cluding p55. Earlier homology searches of the sequence data banks revealed that nitric oxide synthase contains a single DHR segment (3), and we have found that a lymphocyte chemoattractant factor and the dystrophin-associated protein syntrophin (41) also contain DHR segments. Our demonstration that protein 4.1 binds *in vitro* to the hdlg DHR domain provides evidence that this domain functions as a site for protein–protein interaction. Furthermore, preliminary experiments indicate that the hdlg DHR domain associates with at least two proteins in whole cell lysates (data not shown).

Our results also show that a second binding site for protein 4.1 lies between the SH3 and GUK domains of alternatively spliced hdlg isoforms bearing the I3 insertion. The 34-aa long I3 insertion is 38% identical to the analogous region in dlg and may represent another conserved protein-binding domain (Fig. 6*B*). The significance of a distinct subset of hdlg molecules being able to bind protein 4.1 at two sites is unclear, but it is possible that the specificities of the two sites differ, with one having a higher affinity for another protein 4.1-related family member. One site could, for example, facilitate membrane association at regions of cell–cell contact via protein 4.1 while the other is available for interactions with other related proteins. This possibility is consistent with the common subcellular localization of protein 4.1-related family members. Alternatively, a bivalent interaction with protein 4.1 might enable the formation of a physical network of hdlg molecules that could crosslink both protein 4.1 and its associated proteins. The presence of two alternatively spliced protein binding sites, I1 and I3, which bind SH3 domains and protein 4.1, respectively, further suggests that various hdlg isoforms have distinct functions in the cell.

The relationship between negative regulation of cell proliferation and the localization of tumor suppressor proteins at sites of cell–cell contact is not fully understood. In the case of dlg, which localizes at septate junctions, a loss of cell–cell contact in the imaginal discs is an important characteristic of the mutant phenotype (2). Perhaps a causal relationship exists between structural changes in cell–cell contact and the more global event of cell transformation. The evidence we have presented here suggests that dlg-related proteins directly interact with 4.1-related proteins, thus forming a complex between two families of structural and signal-transduction molecules. Indeed, the regulation of this complex at regions of cell–cell contact may dictate how structural proteins contribute to cellular homeostasis.

We thank A. Viel, E. Brandin, and K. Andrabi for their contributions during the early phase of this work and the members of the Branton and Chishti laboratories for helpful discussions. We also thank R. L. Erikson for constructive criticisms, J. L. Strominger for the BM14 lymphocytes, and L. B. Chen for the MCF-7 cells. This work was supported by National Institutes of Health Grants HL17411 (D.B.) and HL51445 and HL37462 (A.H.C.).

1. Woods, D. F. & Bryant, P. J. (1989) *Dev. Biol.* **134**, 222–235.
2. Woods, D. F. & Bryant, P. J. (1991) *Cell* **66**, 451–464.
3. Cho, K.-O., Hunt, C. A. & Kennedy, M. B. (1992) *Neuron* **9**, 929–942.
4. Kistner, U., Wenzel, B. M., Veh, R. W., Cases-Langhoff, C., Garner, A. M., Appeltauer, U., Voss, B., Gundelfinger, E. D. & Garner, C. (1992) *J. Biol. Chem.* **268**, 4580–4583.
5. Willott, E., Balda, M. S., Fanning, A. S., Jameson, B., Van Itallie, C. & Anderson, J. M. (1993) *Proc. Natl. Acad. Sci. USA* **90**, 7834–7838.
6. Itoh, M., Nagafuchi, A., Yonemura, S., Kitani-Yasuda, T., Tsukita, S. & Tsukita, S. (1993) *J. Cell Biol.* **121**, 491–502.
7. Jesaitis, L. A. & Goodenough, D. A. (1994) *J. Cell Biol.* **124**, 949–961.
8. Ruff, P., Speicher, D. W. & Husain-Chishti, A. (1991) *Proc. Natl. Acad. Sci. USA* **88**, 6595–6599.
9. Chomczynski, P. & Sacchi, N. (1987) *Anal. Biochem.* **162**, 156–159.
10. Sambrook, J., Fritsch, E. F. & Maniatis, T. (1989) *Molecular Cloning: A Laboratory Manual* (Cold Spring Harbor Lab. Press, Plainview, NY), 2nd Ed.
11. Gubler, U. & Hoffman, B. J. (1983) *Gene* **25**, 263–269.
12. Smith, D. B. & Johnson, K. S. (1988) *Gene* **67**, 31–40.
13. Sigel, M., Shinha, Y. W. & Vanderlaan, W. P. (1983) *Methods Enzymol.* **93**, 3–12.
14. Lee, J. K., Coyne, R. S., Dubreuil, R., Goldstein, L. S. B. & Branton, D. (1993) *J. Cell Biol.* **123**, 1797–1809.
15. Stehle, T. & Schulz, G. E. (1992) *J. Mol. Biol.* **224**, 1127–1141.
16. Ren, R., Mayer, B. J., Cicchetti, P. & Baltimore, D. (1993) *Science* **259**, 1157–1161.
17. Booker, G. W., Gout, I., Downing, A. K., Driscoll, P. C., Boyd, J., Waterfield, M. D. & Campbell, I. D. (1993) *Cell* **73**, 813–822.
18. Dubreuil, R., Byers, T. J., Branton, D., Goldstein, L. S. B. & Kiehart, D. P. (1987) *J. Cell Biol.* **105**, 2095–2102.
19. Marfatia, S. M., Lue, R. A., Branton, D. & Chishti, A. H. (1994) *J. Biol. Chem.* **269**, 8631–8634.
20. Conboy, J. G., Chan, J. Y., Chasis, J. A., Kan, Y. W. & Mohandas, N. (1991) *J. Biol. Chem.* **266**, 8273–8280.
21. Leto, T. L. & Marchesi, V. T. (1984) *J. Biol. Chem.* **259**, 4603–4608.
22. Ohanian, V. & Gratzer, W. (1984) *Eur. J. Biochem.* **144**, 375–379.
23. Ling, E., Danilov, Y. N. & Cohen, C. M. (1988) *J. Biol. Chem.* **263**, 2209–2216.
24. Metzenberg, A. B. & Gitschier, J. (1992) *Human Mol. Genet.* **1**, 97–101.
25. Berger, A., Schiltz, E. & Schulz, G. E. (1989) *Eur. J. Biochem.* **184**, 433–443.
26. Koonin, E. V., Woods, D. F. & Bryant, P. J. (1992) *Nat. Genet.* **2**, 256–257.
27. Rozakis-Adcock, M., Fernley, R., Wade, J., Pawson, T. & Bowtell, D. (1993) *Nature (London)* **363**, 83–85.
28. Gout, I., Dhand, R., Hiles, I. D., Fry, M. J., Panayotóu, G., Das, P., Truong, O., Totty, N. F., Hsuan, J., Booker, G. W., Campbell, I. D. & Waterfield, M. D. (1993) *Cell* **75**, 25–36.
29. Darbon, H., Bernassau, J.-M., Deleuze, C., Chenu, J., Roussel, A. & Cambillau, C. (1992) *Eur. J. Biochem.* **209**, 765–771.
30. Yu, H., Chen, J. K., Feng, S., Dalgarno, D. C., Brauer, A. W. & Schreiber, S. L. (1994) *Cell* **76**, 933–945.
31. Rees, D. J. G., Ades, S. E., Singer, S. J. & Hynes, R. O. (1990) *Nature (London)* **347**, 685–689.
32. Gould, K. L., Bretscher, A., Esch, F. S. & Hunter, T. (1989) *EMBO J.* **8**, 4133–4142.
33. Gu, M., York, J. D., Warshawsky, I. & Majerus, P. W. (1991) *Proc. Natl. Acad. Sci. USA* **88**, 5867–5871.
34. Trofatter, J. A., MacCollin, M. M., Rutter, J. L., Murrell, J. R., Duyao, M. P., *et al.* (1993) *Cell* **72**, 791–800.
35. Rouleau, G. A., Merel, P., Lutchman, M., Sanson, M., Zucman, J., *et al.* (1993) *Nature (London)* **363**, 515–521.
36. Kaiser, H. W., O'Keefe, E. & Bennett, V. (1989) *J. Cell Biol.* **109**, 557–570.
37. Kupfer, A., Singer, S. J. & Dennert, G. (1986) *J. Exp. Med.* **163**, 489–498.
38. Burn, P., Kupfer, A. & Singer, S. J. (1988) *Proc. Natl. Acad. Sci. USA* **85**, 497–501.
39. Sato, N., Funayama, N., Nagafuchi, A., Yonemura, S., Tsukita, S. & Tsukita, S. (1992) *J. Cell Sci.* **103**, 131–143.
40. Fehon, R. G., Dawson, I. A. & Artavanis-Tsakonas, S. (1994) *Development (Cambridge, U.K.)* **120**, 545–557.
41. Kramarcy, N. R., Vidal, A., Froehner, S. C. & Sealock, R. (1994) *J. Biol. Chem.* **269**, 2870–2876.